DOI 10.5162/irs2017/i2.3

Thermal modulation behavior of infrared emitters with cantilevered heating elements

Tobias Ott, Marco Schossig, Gerald Gerlach
Technische Universität Dresden, Institute for Solid-State Electronics, 01062 Dresden, Germany
tobias.ott@tu-dresden.de

Abstract:
In non-dispersive infrared (NDIR) gas analysis thermal infrared (IR) emitters and pyroelectric sensors are used together to utilize the absorption of IR radiation by gases at characteristic wavelengths. The infrared source has to provide alternating infrared radiation as pyroelectric detectors are only sensitive to changes of radiation and alternating electrical signals can be better processed. Because mechanical choppers prevent the miniaturization of the gas sensor and make the system susceptible, it is necessary to use an electrically modulated IR emitter. Under cyclic excitation the thermodynamic properties of the IR source affect the emitted infrared radiation and, in consequence, the sensor signal. Optimal gas sensor operations (e.g. with regard to gas measurement resolution) require to know which factors influence the thermodynamic properties of thermal emitters.

In this paper an analytical approach is introduced to determine the influence factors on the thermodynamic properties of IR emitters with cantilevered heating elements. The approach is based on the conservation of energy, which means that the electrical input power is completely dissipated into Joule heat, e.g. through radiation and heat conduction. To balance all dissipated heat fluxes, the first law of thermodynamics is applied. Following the Stefan-Boltzmann law the thermal heat flux radiated by the heating element of the IR emitter is dependent upon the fourth power of its thermodynamic (absolute) temperature. Thus, the thermal balance equation is a nonlinear differential equation of first order. As this equation cannot be solved analytically, a numerical solution process is applied. Finally, the model is validated by means of measured heating and cooling temperature curves of an IR emitter.

Key words: thermal emitter, thermal modulation, heating curve, gas analysis, gas measurement

Introduction

Analytic models to describe thermodynamic properties of infrared (IR) emitters are to be found in [1] and [9]. To reproduce the temporary course of heating and cooling curves these models are based on time constants, which are usually used to characterise the thermal modulation behaviour of IR sensors. As shown in this paper, time constants are, however, not appropiate to reproduce the heating and cooling curves of IR emitters. This follows from the fact, that the radiation in the analytic model of IR sensors is neglectable, while for IR emitters it is not anymore because of high element temperatures. As a result, the differential equation to describe the thermal behaviour of IR emitters is highly nonlinear.
The knowledge to determine the thermodynamic properties of IR emitters offers a multitude of optimisation possibilities in the field of NDIR gas analysis. In the field of NDIR gas analysis the trend is towards miniaturisation and low energy consumption of gas measurement devices. In consequence, these devices require energy-efficient IR emitters. By variation of the parameters of the thermal model the heating and cooling curves of IR emitters can be reproduced. Now, extensive statements about thermal losses of the emitter can be made and may be optimised.
The insight into the thermal conditions of the IR emitter allows the reduction of thermal losses, e.g. by customisation of the heating element design or by using alternative gas fillings. Such an optimised IR emitter can be used in gas measurement devices of small size

- to monitor indoor air quality (e.g. detection of CO and CO_2),
- for smoke and fire detection (CO, CO_2) as well as
- to recognise gas leakage (detection of coolants and nitrogen oxides)

(see [11], [12] and refs. therein).

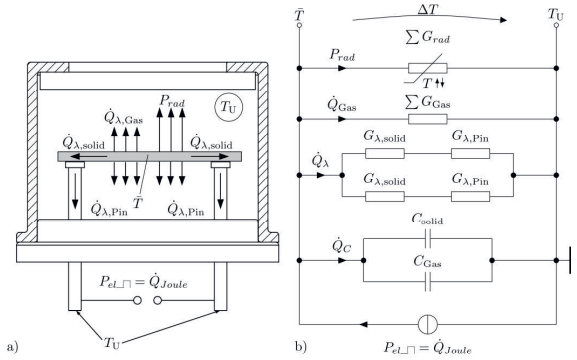

Fig. 1. a) Input power and dissipated heat fluxes of an iR emitter in a TO housing. b) Thermal resistor model of the IR source. $\sum G_i = G_{i,top} + G_{i,bot}$, $i \in rad, \mathrm{Gas}$ *The heating conductor has a top and bottom area. Both areas are used to emit radiation and conduct heat through the filling gas.*

Model of a thermal IR emitter

The thermal model of the IR emitter is inspired by *Schulz et al.* [1]. Fig. 1 shows the thermal conditions of the heating element in a TO housing. The input power P_{el} is converted completely into Joule heat, which is dissipated into the environment through

- radiation P_{rad},
- solid-state heat conduction within the heating conductor ($\dot{Q}_{\lambda,\mathrm{solid}}$) and the header-pins ($\dot{Q}_{\lambda,\mathrm{Pin}}$) as well as
- overall heat transfer ($\dot{Q}_{\mathrm{Gas}}$) consisting of conduction and convection through the filling gas.

For the system in Fig. 1, the first law of thermodynamics from [2, p. 108] was taken into consideration:

$$\left(C_{\mathrm{solid}} + C_{\mathrm{Gas}}\right) \frac{\mathrm{d}\Delta T}{\mathrm{d}t} = P_{el} - \left(P_{rad} + \dot{Q}_{\lambda} + \dot{Q}_{\mathrm{Gas}}\right) \tag{1}$$

with C being the heat capacity, P_{el} the electrical input power, P_{rad} the radiant power and $\dot{Q}$ the discharged heat flux.

The differential of a sum is equal to the sum of differentials of the terms and the differential of a constant is zero [3, p. 116]:

$$\frac{\mathrm{d}\Delta T}{\mathrm{d}t} = \frac{\mathrm{d}T}{\mathrm{d}t} - \underbrace{\frac{\mathrm{d}T_{\mathrm{U}}}{\mathrm{d}t}}_{=0} = \frac{\mathrm{d}T}{\mathrm{d}t}. \tag{2}$$

Using the incremental resistance analogous to electrical engineering [1; 4, p. 20], for the heat flux applies:

$$\frac{\mathrm{d}\dot{Q}}{\mathrm{d}T} = G_{th} \;\Rightarrow\; \dot{Q} = \int G_{th} \mathrm{d}T. \tag{3}$$

The radiation conductance is generally defined by:

$$G_{rad} = \frac{\mathrm{d}P_{rad}}{\mathrm{d}T} = \frac{\mathrm{d}\left(\varepsilon\sigma A_{\mathrm{emit}} T^4\right)}{\mathrm{d}T} = 4\varepsilon\sigma A_{\mathrm{emit}} T^3. \tag{4}$$

The value ε stands for the broadband emissivity, σ is the Stefan-Boltzmann constant and A_{emit} the emitting area of radiation.

For the thermal conductance it generally applies that

$$G_i = \frac{\lambda_i A_i}{\delta_i}, \tag{5}$$

with the thermal conductivity λ_i as well as the cross section A_i and the length δ_i of the thermally conductive path.

Generally, the heat capacity C can be determined with

$$C_i = c_i \varrho_i V_i \tag{6}$$

with c_i being the specific heat capacity, ϱ_i being the density and V_i being the volume of the heated body.

Inserting Eq. (3) in Eq. (1), the rearranged thermal balance equation is as follows:

$$\left(C_{\mathrm{solid}} + k_C C_{\mathrm{Gas}}\right) \frac{\mathrm{d}\bar{T}}{\mathrm{d}t} + \int_{T_{\mathrm{U}}}^{\bar{T}} \left(G_{rad} + G_{\lambda} + k_{conv} G_{\mathrm{Gas}}\right) \mathrm{d}T = P_{el}\left(t, f_m\right) \tag{7}$$

with the mean absolute temperature $\bar{T}$, the ambient temperature T_{U}, the heat capacity of the heating conductor C_{solid} and of the gas filling C_{Gas}, the radiation conductance G_{rad}, the thermal conductances of the heating conductor G_{λ} and the gas filling G_{Gas} as well as the electrical input power P_{el} with square waveform and modulation frequency f_m. To adapt the model to reality, the parameters k_{conv} and k_C are introduced. The factor $k_{conv} > 1$ takes account of the heat flux dissipated through convection in addition to the heat flux dissipated through thermal conductance in the filling gas. With respect to the non-uniform heating of the gas volume $k_{\mathrm{C}} < 1$ is introduced.

Eq. (7) is a highly nonlinear differential equation of first order. For this type of equation a thermal time constant is not appropriate, because it is only reasonable for first-order linear differential equations reacting to the Heaviside step function. There is no analytical solution for this type of equation, hence the equation is solved numerically.

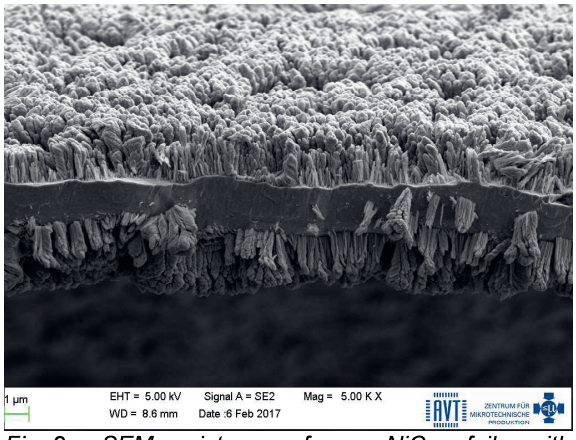

Fig. 2. SEM picture of a NiCr foil with nanostructured NiCr emission layers.

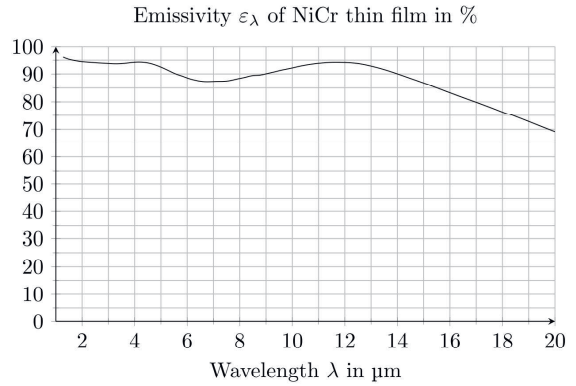

Fig. 3. Measured spectral emissivity of NiCr emission layer.

Numerical results are obtained with a Runge Kutta 4th order method described in [6, pp. 132 ff.]. For this purpose Eq. (7) is rearranged for $\frac{\mathrm{d}\bar{T}}{\mathrm{d}t} = f\left(t, \bar{T}\right)$ and solved numerically for $\bar{T}\left(t\right)$ with the starting conditions $t_0 = 0\,\mathrm{s}$ and $\bar{T}_0 = T_\mathrm{U}$.

Experimental and numerical results

The heating and cooling curves are measured at the NiCr heating conductor in a TO8 housing of 1.5 mm width with a pyrometer (see Fig. 4). The measuring spot of the pyrometer is 0.7 mm in diameter and the sampling frequency of the temperature measurement is about 400 Hz. The spectral range of the pyrometer is (3...5) µm and the lowest measurable temperature is 60 °C. At the top and bottom side of the heating conductor porous layers (Fig. 2) of NiCr are applied to increase the spectral emissivity (Fig. 3). To measure the temperature of the heating conductor, the emissivity value of the pyrometer has to be set correctly. This emissivity value is the product of the band emissivity of the NiCr layer and the mean band transmission of the CaF_2-window. The band emissivity $\varepsilon_{(3\ldots5)\mu\mathrm{m}}\left(T\right)$ has to be determined by means of [5, Eq. 2.2.33] with the measured spectral emissivity.

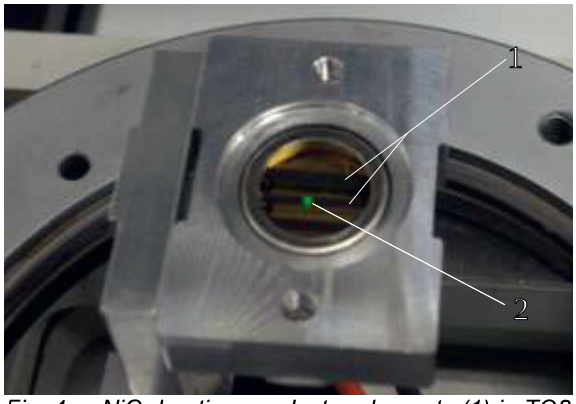

Fig. 4. NiCr heating conductor elements (1) in TO8 housing with CaF_2-window and pyrometer spot (2).

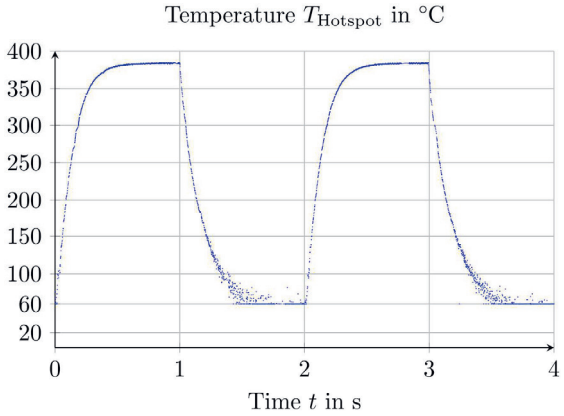

Fig. 5. Temporary course of measured heating conductor temperature for low modulation frequency of $f_m = 0.5\,\mathrm{Hz}$.

The band emissivity has a low temperature dependency, hence its mean value is $\bar{\varepsilon}_{(3\ldots5)\mu\mathrm{m}} \approx 0.94$. The mean band transmission of the CaF_2-window was determined as $\bar{\tau}_{\mathrm{CaF_2}(3\ldots5)\mu\mathrm{m}} \approx 0.94$.

The measurement result is shown in Fig. 5. If the measured temperature approaches the lower end of the measurement range of 60 °C the signal-to-noise ratio is reduced so far, that the signal is superimposed with noise.

To reproduce the measured heating and cooling curves, the analytical model requires optical and physical properties of the NiCr emission layers, material properties of the NiCr heating conductor and the emission layers, material properties of the filling gas Argon as well as the dimensions of the heating conductor and the TO8 housing to determine the cross section and the length of the thermally conductive paths in Eq. (5).

To perform the integration of the radiation conductance in Eq. (7) the broadband emissivity of the NiCr layer is used.

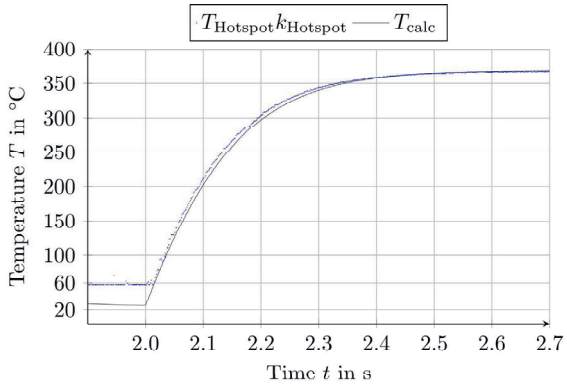

Fig. 6. Measured ($T_{\mathrm{Hotspot}} k_{\mathrm{Hotspot}}$) and calculated ($T_{calc} = \bar{T}$) temporary course of the heating curve.

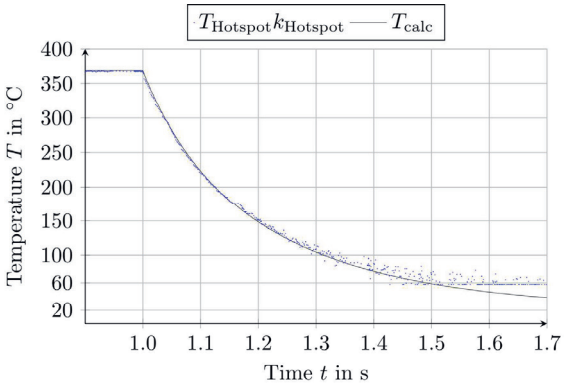

Fig. 7. Measured ($T_{\mathrm{Hotspot}} k_{\mathrm{Hotspot}}$) and calculated ($T_{calc} = \bar{T}$) temporary course of the cooling curve.

This value is calculated with [5, Eq. 2.2.33] and the spectral emissivity of Fig. 2. This emissivity has a low temperature dependency as well, therefore its mean value $\varepsilon = 0.89$ is used. For identical top and bottom emission layers, the overall emitting area adds up to $\sum A_{\mathrm{emit}} = 2 \cdot 15\ \mathrm{mm}^2$.

The heating conductor is heated to a maximum temperature of about $400\ ^{\circ}\mathrm{C}$ during the measurement. The material properties of the filling gas and the heating conductor are temperature-dependent. To simplify the calculation, temperature-independent mean values in the temperature range of $T_{\mathrm{U}} = 20\ ^{\circ}\mathrm{C}$ to $T_{\max} = 400\ ^{\circ}\mathrm{C}$ are used.

The heating conductor is 10 mm long, 1.5 mm wide and 2 µm in thickness. Each one of the double-sided emission layers is 2 µm in thickness and has a porosity of about 50 % [10, p. 97]. With the density of NiCr $\varrho_{\mathrm{NiCr}} = 8.3\ \mathrm{g/cm}^3$ [8, p. 8] and the mean specific heat capacity $c_{p,\mathrm{NiCr}} \approx 435\ \mathrm{J/kg\ K}$ [8, p. 8] in the measurement range the heat capacity $C_{\mathrm{NiCr}} \approx 216\ \mu\mathrm{J/K}$ of the overall heating conductor results.

Furthermore for the thermal conductances of the heating conductor, it results $\sum G_{\lambda} = 19.2\ \mu\mathrm{W/K}$ with the mean thermal conductivity $\lambda_{\mathrm{NiCr}} = 16\ \mathrm{W/(m\ K)}$ [7, p. 313] of NiCr. For Eq. (5) the cross section of the heating conductor and the thermally conductive path $l_{\lambda} = 5\ \mathrm{mm}$ is used. This path is assumed to be the distance from the hotspot of the heating conductor (midway of the heating element) to the header pins, which act as heat sink. The thermal conductance through header pins is neglected.

To calculate the thermal conductivity value of the filling gas, the thermally conductive paths have to be considered. These paths are assumed to be the distance $\delta_{bot} = 2\ \mathrm{mm}$ from the heating element to the bottom of the TO8 housing for $G_{\mathrm{Gas},bot}$ and the distance $\delta_{top} = 1.8\ \mathrm{mm}$ from the heating element to the IR window for $G_{\mathrm{Gas},top}$. Using the mean thermal conductivity $\lambda_{\mathrm{Ar}} = 0.25\ \mathrm{W/(m\ K)}$ [4, p. 376] of Argon and the emitting area $A_{\mathrm{emit}} = 15\ \mathrm{mm}^2$ of the heating conductor the result is $\sum G_{\mathrm{Gas}} \approx 395\ \mu\mathrm{W/K}$.

The filling gas Argon (molecular mass $M_{\mathrm{Ar}} = 39.95\ \mathrm{g/mol}$) is filled up under laboratory conditions ($p = 1013\ \mathrm{mbar}$, $\vartheta = 20\ ^{\circ}\mathrm{C}$), thus having a density of $\varrho_{\mathrm{Ar}} = 1.66\ \mathrm{kg/m}^3$. During heating and cooling of the heating conductor the gas proceeds an isochoric change. With the isochoric heat capacity $c_{v,\mathrm{Ar}} = 312\ \mathrm{J/kg\ K}$ [4, p. 344], and the volume of the gas in the TO8 cap of diameter $d_{\mathrm{Cap}} = 13\ \mathrm{mm}$ and height $h_{\mathrm{Cap}} = 3.8\ \mathrm{mm}$ it results that $C_{\mathrm{Ar}} \approx 261\ \mu\mathrm{J/K}$.

Figs. 6 and 7 show the superposition of the measured (from Fig. 5) and calculated temporary courses of the heating conductor temperatures. The measured temperature is the temperature of the hotpsot of the heating conductor. The analytical model calculates a mean temperature $\bar{T}$ of the heating conductor. For the superposition of both curves, the hotspot temperature is converted into mean temperature with the factor

$$k_{\mathrm{Hotspot}} = \bar{T} \ / \ T_{\mathrm{Hotspot}}. \tag{8}$$

This factor is measured with the pyrometer on different positions of the heating conductor under direct current with subsequent averaging.

From the analytical model it follows $k_{conv} = 4.1$ and $k_{\mathrm{C}} = 0.6$. This means, that the heat flux through the filling gas is about four times higher in contrast to pure heat conduction. Consequently, the convection is about three times higher than heat conduction through the filling gas. This fact allows to conclude, that the majority of the heat flux through the filling gas in

this TO8 housing is conducted through convection. Because of the non-uniformity of the heating and cooling of the gas volume it follows $k_{\mathrm{C}} < 1$. The effective heat capacity of Argon $C_{\mathrm{Ar},eff} = k_C C_{\mathrm{Ar}}$ lies in the order of the heat capacity of the heating conductor, thus, it is not negligible.

Conclusion and Outlook

The heating and cooling curves of a cantilevered heating conductor has been reproduced analytically. The heat flux conducted through the filling gas is about four times higher compared to pure heat conduction. This fact leads to the conclusion, that the convection has a dominant influence on the conducted heat flux through the filling gas in the studied case with the TO8 housing. In addition, the heat capacity of the filling gas contributes substantially to the thermal inertia of the IR emitter and must not be neglected.

Measurements performed in vacuum should support the statements made in this paper regarding the influence of the filling gas on the thermal behaviour of the IR emitter. Furthermore, the definition of thermodynamic properties of IR emitters would go beyond the scope of this paper and is therefore subject of another publication.

Acknowledgement

The authors would like to thank the German Research Foundation (DFG) for supporting this work under grant number GE 779/32.

References

[1] O. Schulz, G. Müller, M. Lloyd, and A. Ferber, “Impact of environmental parameters on the emission intensity of micromachined infrared sources”, *Sensors and Actuators A: Physical* 121.1 (2005): 172–180, doi: 10.1016/j.sna.2004.12.010.

[2] H. D. Baehr and K. Stephan, *Heat and Mass Transfer*. Springer Berlin, Heidelberg, 2011, doi: 10.1007/978-3-642-20021-2.

[3] V. I. Smirnov, A Course of Higher Mathematics, vol. 1, vol. 57 of *Pergamon Press International Series of Monographs in Pure and Applied Mathematics*. Pergamon Press Oxford, London et al., 1964.

[4] M. Kind and H. Martin, *VDI Heat Atlas*. Springer-Verlag Berlin Heidelberg, 2010, doi: 10.1007/978-3-540-77877-6.

[5] H. Budzier and G. Gerlach, *Thermal Infrared Sensors: Theory, Optimisation and Practice*. John Wiley & Sons, 2011, doi: 10.1002/9780470976913.ch6.

[6] E. Hairer, S. P. Nørsett, and G. Wanner, *Solving Ordinary Differential Equations I: Nonstiff Problems*, 2nd ed., Springer, Berlin, Heidelberg, 1993, doi: 10.1007/978-3-540-78862-1.

[7] G. Neuer, “Ni-based alloys: Thermal Conductivity of Pure Metals and Alloys,” in *Landolt-Börnstein - Group III Condensed Matter*, vol. 15C, O. Madelung and G. K. White, Eds. Springer-Verlag, Berlin, Heidelberg, 1991, 306–320, doi:10.1007/10031435_58.

[8] DIN 17470, *Heizleiterlegierungen - Technische Lieferbedingungen für Rund- und Flachdrähte*. Deutsches Institut für Normung, 1984.

[9] J. Spannhake, “Hochtemperaturstabile Mikroheizer für miniaturisierte Sensorsysteme.” Dissertation, TU Ilmenau, Univ.-Verl. Ilmenau, Ilmenau, 2009.

[10] M. Schossig, Ultradünne, freitragende Lithiumtantalat-Elemente für hochdetektive Infrarotsensoren. Dissertation, TU Dresden, TUDpress, 2012.

[11] J. Y. Wong and R. L. Anderson, *Non-Dispersive Infrared Gas Measurement*. International Frequency Sensor Association Publishing, 2012.

[12] J. Zosel, W. Oelßner, M. Decker, G. Gerlach, and U. Guth, “The measurement of dissolved and gaseous carbon dioxide concentration”, Measurement Science and Technology 22.7 (2011), 72001, doi: 10.1088/0957-0233/22/7/072001